

Nonmonotonic evolution of the charge gap in ZnV_2O_4 under pressure

Christine Kuntscher,¹ Kaneez Rabia,¹ M. K. Forthaus,² M. M. Abd-Elmeguid,² F. Rivadulla,³ Y. Kato,⁴ and C. D. Batista⁴

¹*Experimentalphysik 2, Universität Augsburg, D-86135 Augsburg, Germany*

²*II. Physikalisches Institut, Universität zu Köln, D-50937 Köln, Germany*

³*Centro de Investigacion en Química Biológica y Materiales Moleculares (CIQUS), Universidad de Santiago de Compostela, 15782 Santiago de Compostela, Spain*

⁴*Theoretical Division, T-4 and CNLS, Los Alamos National Laboratory, Los Alamos, New Mexico 87545, USA*

(Received 11 May 2012; revised manuscript received 20 June 2012; published 20 July 2012)

$\text{A}^{2+}\text{V}_2\text{O}_4$ spinels provide a unique opportunity for studying the evolution of the charge gap of Mott insulators that approach the itinerant electron limit under the application of external pressure. Here we report high-pressure resistivity and optical measurements in ZnV_2O_4 that provide unambiguous evidence of an unusual nonmonotonic behavior of the charge gap, Δ , as a function of pressure P . These unexpected results suggest that ZnV_2O_4 undergoes a crossover from a Mott insulator with a charge gap dominated by the on-site Coulomb repulsion U , to a second type of insulator in the high pressure regime. Our Monte Carlo simulations of the three-band Hubbard model relevant for ZnV_2O_4 reproduce the nonmonotonic behavior of $\Delta(P)$ and provide a partial understanding of this exotic phenomenon.

DOI: [10.1103/PhysRevB.86.020405](https://doi.org/10.1103/PhysRevB.86.020405)

PACS number(s): 72.80.Sk, 75.25.Dk, 75.85.+t

Mott insulators are paradigmatic examples of strongly correlated materials. Electronic charge localization is driven by a strong intra-atomic Coulomb repulsion, U , that prevents valence electrons from occupying the same orbital. This contribution competes against the kinetic energy term that favors electronic delocalization: electrons can hop with an amplitude t between valence orbitals of nearest-neighbor ions. The strong-coupling limit, $U \gg t$, corresponds to materials in which valence electrons are strongly localized in their atomic orbitals. Since the charge is “quasifrozen” in this limit, the effective low-energy degrees of freedom are the orbital flavor and the localized magnetic moments that arise from the single-occupancy condition (unpaired electronic spins). The opposite weak-coupling limit, $U \ll t$, corresponds to correlated metals whose electrons are completely delocalized. This simple analysis implies that a metal-insulator or Mott transition is induced at a critical value U_c/t . One of the current experimental and theoretical challenges in condensed matter physics is the characterization of the electronic properties when approaching the Mott transition.

Many fascinating properties of doped high- T_C cuprates and CMR manganites are influenced by their proximity to a Mott transition, with a characteristic intermixing of orbital, spin, and charge degrees of freedom. In general, there are few examples of simple materials whose t/U ratio can be varied under control. The $\text{A}^{2+}\text{V}_2\text{O}_4$ spinels are a family of Mott insulators that fulfill this criterion because the V-V distance can be reduced significantly by decreasing the size of the A^{2+} cation.¹ The absence of e_g electrons makes direct V-V hybridization between t_{2g} orbitals the only relevant contribution to the hopping amplitude. Therefore, reducing the bond-distance increases t/U .

ZnV_2O_4 has one of the smallest charge gaps among the vanadium spinels: ($\Delta \simeq 0.55$ eV).^{2,3} It is then expected that moderate pressures should be enough to reach the Mott transition for this material. In contrast to this naive expectation, the resistivity and optical measurements of $\Delta(P)$ that we report in this Rapid Communication show clear evidence of a nonmonotonic behavior ($\Delta(P)$ reaches the minimum value

near 11 GPa). This unusual phenomenon suggests the existence of a crossover between two different insulating regimes: a low-pressure Mott phase, whose gap is induced by the on-site electronic repulsion U , and a high-pressure regime with a charge gap induced by a different mechanism. The measured nonmonotonic dependence of Δ on t/U is reproduced by our quantum Monte Carlo simulations of the three-orbital Hubbard Hamiltonian relevant for ZnV_2O_4 . Our theoretical results indicate that the change of sign of $d\Delta/dP$ is accompanied by a suppression of the orbital ordering expected for materials that are deep inside the Mott regime (small t/U ratio)^{4,5} and the enhancement of the magnetic up-up-down-down ordering along the $[\pm 1, 0, 1]$ and $[0, \pm 1, 1]$ chains that has been reported in these materials.⁶

Single-phase, polycrystalline ZnV_2O_4 spinel was synthesized by solid-state reaction from stoichiometric V_2O_3 and dried ZnO in evacuated quartz ampoules. Structural parameters were derived from x-ray diffraction patterns by Rietveld analysis. Resistivity under pressure was measured in a diamond anvil cell (DAC), using a mixture of epoxy and Al_2O_3 for the pressure-transmitting medium. Pressure was determined by using the ruby fluorescence method.⁷ Energy dispersive x-ray diffraction data under pressure at room temperature were recorded at HASYLAB, Hamburg, beamline F3, using a DAC and liquid nitrogen as the pressure-transmitting medium. Here, pressure was determined with a gold calibrant inside the sample chamber that allows for *in situ* determination of the pressure from the known lattice parameter of gold⁸ and the Murnaghan equation of state.⁹ Pressure-dependent transmittance experiments were conducted at room temperature by using a Bruker IFS 66v/S FT-IR spectrometer with an infrared microscope (Bruker IRscope II), and a DAC,¹⁰ using CsI powder as pressure transmitting medium. The applied pressure P was determined with the ruby luminescence method.⁷ The transmittance spectrum was obtained by measuring the intensity $I_s(\omega)$ of the radiation transmitting through the sample [$T(\omega) = I_s(\omega)/I_r(\omega)$], while the corresponding absorbance was calculated according to $A = \log_{10}(1/T)$, where A is a measure of the real part of the optical conductivity.

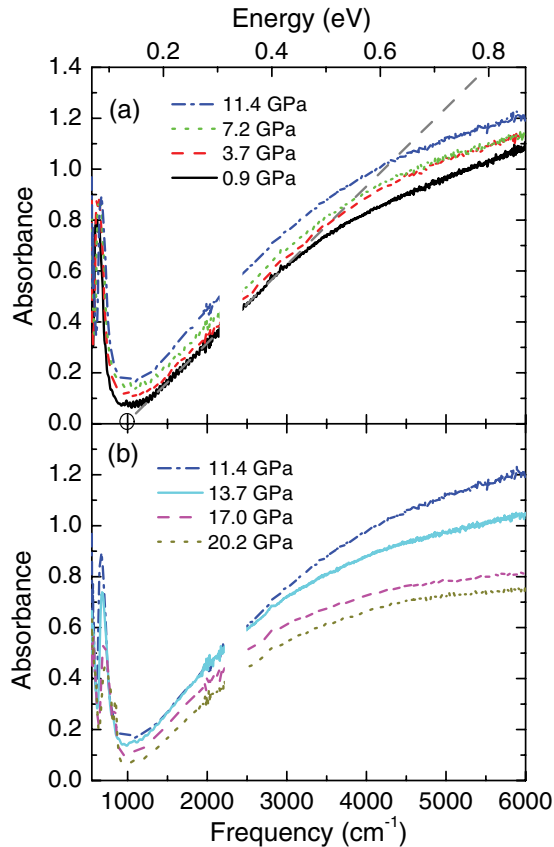


FIG. 1. (Color online) Room temperature absorbance spectra of ZnV_2O_4 in the midinfrared range for the low-pressure (a) and high-pressure (b) regime. The dashed gray line in (a) is the linear extrapolation used to determine the absorption edge (intersection of the linear extrapolation with the frequency axis marked by an open circle) at the lowest pressure (0.9 GPa).

Figure 1 shows the absorbance spectrum of ZnV_2O_4 in the midinfrared range. The peak observed below $\approx 1000 \text{ cm}^{-1}$ corresponds to one of the four phonon modes expected for cubic spinels. The absorbance spectra show a strong onset above $\approx 1000 \text{ cm}^{-1}$, with a totally unexpected behavior as a function of pressure: the absorption edge shifts to lower energies for increasing pressures below $P_c \sim 11 \text{ GPa}$ [Fig. 1(a)], while the opposite trend is observed for $P \geq P_c$ [Fig. 1(b)]. The charge gap $\Delta(P)$ is estimated from the intersection of the linear extrapolation of the absorption edge and the frequency axis, as it is illustrated in Fig. 1(a). Δ decreases with pressure up to $P_c \sim 11 \text{ GPa}$, and it starts increasing above this threshold value producing a clear minimum in the $\Delta(P)$ curve (see Fig. 2).

To confirm the validity of these results, we measured the temperature dependence of the electrical resistivity of ZnV_2O_4 up to 17.4 GPa. The temperature range available for the fittings is wide enough because the resistance becomes too large only below 150 K. The activation energy extracted from the $\ln R$ vs $1/T$ plots shows a clear minimum at $P_c \sim 8(2) \text{ GPa}$. The discrepancy between the P_c value extracted from the transport and optical data could be related to the influence of intergrain scattering to the resistivity in a polycrystalline sample. In spite of this quantitative disagreement, both techniques show the same nonmonotonic dependence of the gap as a function of P .

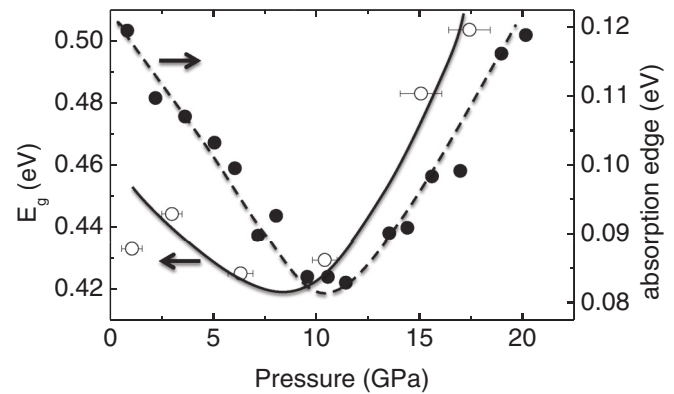


FIG. 2. Pressure dependence of the activation energy obtained from the fittings of the R vs T curves (open symbols), and from the position of the absorption edge (closed symbols).

Further indications of a pressure-induced instability are found in the measured phonon spectrum of ZnV_2O_4 . Figure 3 shows a blowup of the low-frequency region of Fig. 1, which contains the highest-frequency phonon that will be called “phonon mode 4” from now on. Although the phonon excitation is quite broad already at the lowest pressure, a threefold splitting is clearly visible for $P_c \gtrsim 12 \text{ GPa}$ (see Supplemental Material).¹¹ This observation suggests a pressure induced structural phase transition ZnV_2O_4 .

To analyze the origin of the pressure-induced transition, it is important to review the original structure at ambient pressure. ZnV_2O_4 undergoes a structural transition at $\approx 50 \text{ K}$ from the high temperature cubic $Fd\bar{3}m$ to the low temperature tetragonal phase $I4_1/amd$.¹² It has been proposed recently that this transition is induced by partial electronic delocalization due to the proximity of ZnV_2O_4 to the Mott transition.² The band structure calculation presented in Ref. 2 indicates that V-V dimers form along the [011] and [101] directions together with an $\uparrow\uparrow\downarrow\downarrow$ magnetic order along the same directions. The shorter V-V dimers are ferromagnetic and the dimer ordering provides a way of partially releasing the geometric frustration

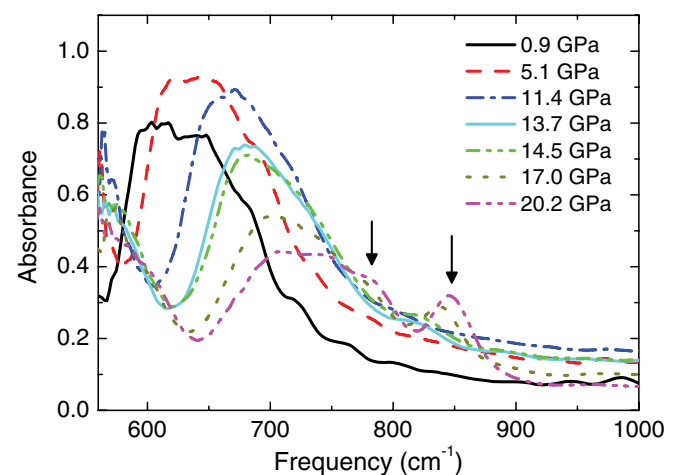


FIG. 3. (Color online) Low-frequency part of Fig. 1 showing the highest-frequency phonon mode (phonon mode 4). The threefold splitting of this phonon mode with increasing pressure is indicated by the arrows, for the highest pressure (20.2 GPa).

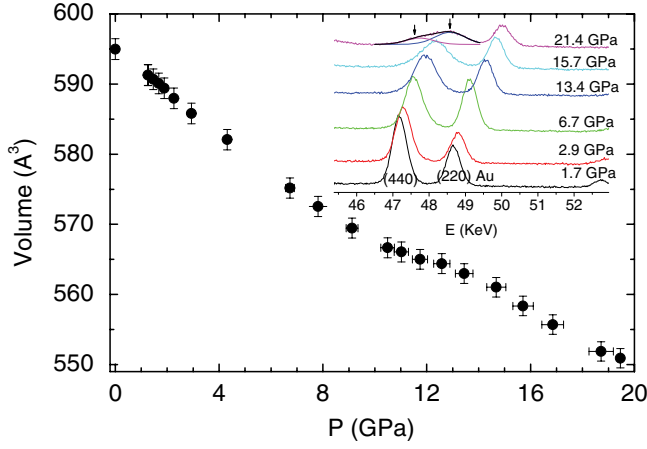


FIG. 4. (Color online) Pressure dependence of the lattice volume $V(p)$ of ZnV_2O_4 at room temperature for pressures up to 20 GPa which shows an anomaly in $V(p)$ around 10–12 GPa. The inset shows the (440) Bragg reflection of ZnV_2O_4 and the (220) Bragg reflection of Au which is used as pressure calibrant. The splitting of the cubic (440) reflection of ZnV_2O_4 into tetragonal (400) and (224) reflections is clearly visible for pressures above 20 GPa.

of the spinel structure. It has been shown recently that the same dimer ordering in CdV_2O_4 leads to a ferroelectric distortion¹³ that reduces the crystal symmetry group from $I4_1/amd$ to $P4_12_12$. Figure 4 shows the high-pressure synchrotron data, where an anomaly in the pressured dependence of the sample volume is clearly visible at $P_c \sim 10$ GPa. The splitting of the cubic (440) peak observed in the inset to Fig. 4 is consistent with the appearance of the (400) and (224) peaks of the tetragonal phase $P4_12_12$. Hence the pressure induced structural instability seems to be related to a stabilization of the dimerized phase above $P_c \approx 10$ –12 GPa. Moreover, measurements of the magnetic susceptibility as a function of pressure show that the single magnetostructural transition into the $\uparrow\uparrow\downarrow\downarrow$ ordered phase (with $T_N \simeq 38$ K at ambient pressure) splits into two different transitions above a rather low pressure of 2 kbar.¹

Since the dimerized state is induced by the electronic degrees of freedom, we will consider a purely electronic model of ZnV_2O_4 , although a complete description of the unusual pressure-induced behavior requires a model that also includes the lattice degrees of freedom. We will then consider a three-band Hubbard model that only includes the three low-energy t_{2g} orbitals. The e_g orbitals can be omitted because the octahedral crystal field splitting between e_g and t_{2g} orbitals is of order 2 eV, i.e., much larger than the typical values of the hopping amplitude t between t_{2g} orbitals of nearest-neighbor ions. The corresponding multiorbital Hubbard Hamiltonian is

$$\begin{aligned} \mathcal{H} = & -t \sum_{\sigma,\alpha,(i,j)\parallel\alpha} (d_{i\alpha\sigma}^\dagger d_{j\alpha\sigma} + d_{j\alpha\sigma}^\dagger d_{i\alpha\sigma}) + U \sum_{i,\alpha} n_{i\alpha\uparrow} n_{i\alpha\downarrow} \\ & + (U - 2J) \sum_{i,\alpha\neq\beta,\sigma,\sigma'} n_{i\alpha\sigma} n_{i\beta\sigma'} - J \sum_{i,\alpha\neq\beta,\sigma} n_{i\alpha\sigma} n_{i\beta\sigma} \\ & + \Delta_{cf} \sum_{i,\alpha=\{yz,zx\},\sigma} n_{i\alpha\sigma} - \mu \sum_i n_i, \end{aligned} \quad (1)$$

where $n_{i\alpha\sigma} \equiv d_{i\alpha\sigma}^\dagger d_{i\alpha\sigma}$, $n_i \equiv \sum_{\alpha,\sigma} n_{i\alpha\sigma}$ is the particle density operator, Δ_{cf} is the tetragonal crystal field splitting, and μ is the chemical potential. The off-diagonal terms of the Hund's coupling have been eliminated because they do not play an important role, as long as the magnetic ordering is collinear,⁶ and such terms introduce a negative sign problem. As it is clear from the first term of \mathcal{H} , an electron can hop along an α bond (bond parallel to the α direction) *only when* it occupies an α orbital ($\alpha = \{xy, xz, yz\}$). This is a good approximation as long as the σ bond gives the dominant contribution to the hopping amplitude between nearest-neighbor V^{3+} ions. This hypothesis is indirectly confirmed by the measured Bloch parameter in the more localized vanadium spinel CdV_2O_4 : $\partial T_N / \partial V \simeq 3.3$ ¹ (T_N is the Néel temperature and V is the sample volume). On the other hand, electrons on different orbitals (chains) interact via direct Coulomb and Hund's interactions.

To compute equilibrium properties of \mathcal{H} we apply a quantum Monte Carlo (QMC) method based on the Feynman path integral formulation.¹⁴ In general, three-dimensional fermionic problems cannot be simulated with this method because of the well-known sign problem. However, the sign problem can be eliminated in our case because the electrons can only move along chains oriented in the xy , yz , and zx directions and the interaction terms of \mathcal{H} are all diagonal.¹⁵ The simulations have been performed in finite lattices of L^3 sites with $L = 4, 8, 12$ and closed boundary conditions. More details about the characteristics of this QMC simulation will be presented elsewhere.¹⁶

The charge gap, Δ , was estimated from the width of the plateau in the $\mu(n)$ curve ($n = \sum_i \langle n_i \rangle / L^3$) computed for different values of t/U , with $J = 0.8$ (eV) and $U = 3.9$ (eV) [see Fig. 5(a)]. We use the value $J = 0.8$ eV, which is the average between the values $J = 0.9$ eV given in Ref. 17 and $J = 0.7$ eV from Ref. 18. The value of $U = 3.9$ eV is within the range $U < 4$ eV proposed by Pardo *et al.*² Figure 5(b) shows the t/U dependence of Δ . The clear nonmonotonic behavior as a function of increasing t/U is in qualitative agreement with the pressure dependence that we have extracted from our optical and transport measurements. Although we present results for a range of t/U values that is much wider than the experimentally accessible window, the minimum value of the gap is obtained for $t_c/U \simeq 0.12$ and such value can be slightly above the ratio that is expected for ZnV_2O_4 ($t/U \simeq 0.1$ for $t \simeq 0.35$ eV and $U \simeq 3.5$ eV).⁵ Our QMC simulations also reproduce the observed magnetostructural transition into the above mentioned $\uparrow\uparrow\downarrow\downarrow$ ordered phase. It is important to remark that the measured magnetic ordering is reproduced by using an unbiased (QMC) approach. Moreover, the corresponding ordering temperature increases significantly for $t/U > t_c/U$ indicating that the change in slope of $\Delta(t/U)$ is correlated with a strengthening of the observed magnetostructural ordering at ambient pressure. However, our QMC simulation does not reproduce the splitting between the magnetic and structural transitions that is already observed at low pressures.¹ We believe that this discrepancy is originated in two oversimplifications of our model. In the first place, we are not including the electron-phonon coupling that is relevant for strengthening the dimer ordering in the absence of magnetic ordering. In the second place, we are introducing an artificial easy-axis anisotropy by neglecting the off-diagonal terms of

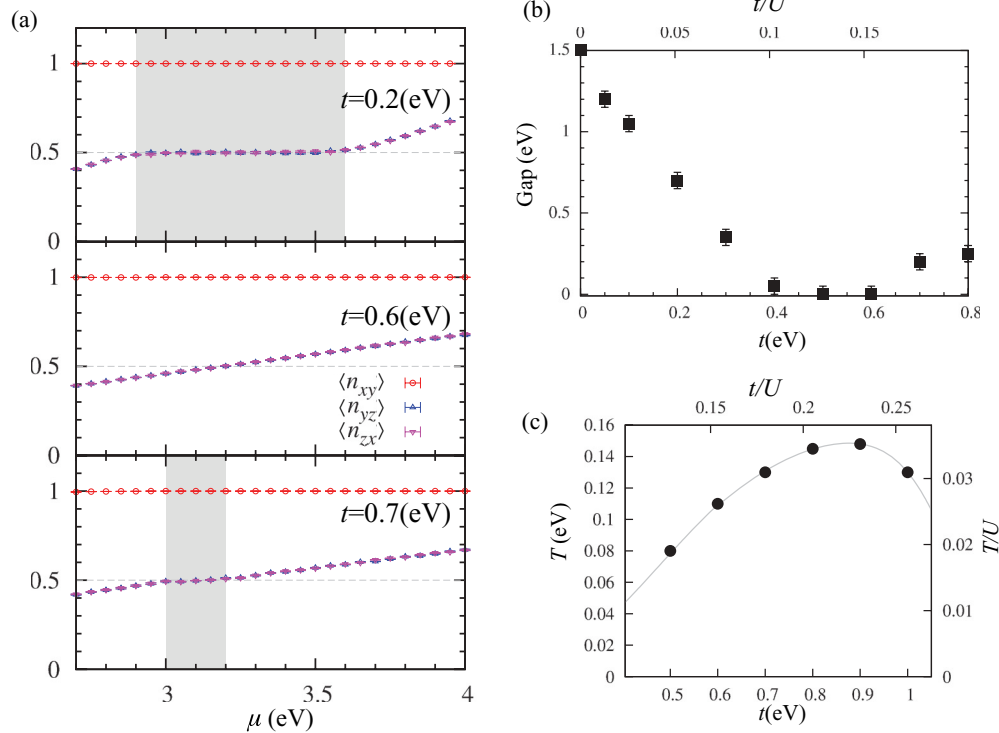


FIG. 5. (Color online) (a) QMC results for the average charge densities in each t_{2g} orbital as a function of chemical potential μ for different values of t , $J = 0.8$ (eV), and $U = 3.9$ (eV). The temperature was fixed at $T = 0.05$ (eV) and we set $\Delta = 1.0$ (eV) so that xy orbital mainly is occupied by one electron and the other electron occupies the yz or zx orbitals. Charge gap as a function of t/U extracted from the $\rho(\mu)$ curves is shown in panel (b). Error bars indicate uncertainty due to the finite temperature. (c) Néel temperature as a function of t/U for $\mu = 3.05$ eV.

the Hund's coupling (our Hund's interaction is Ising-like instead of Heisenberg-like). The consequent reduction of spin fluctuations can also preclude the splitting between the structural and magnetic transitions. Finally, it is important to note that the range of t/U values considered in our QMC simulations (see Fig. 5) is much wider than the range that can be experimentally accessed by applying pressure.

Our experimental observations and numerical calculations suggest that the nonmonotonic dependence of the charge gap is then induced by a transition from a Mott regime, whose charge gap is dominated by the Coulomb repulsion U , to a dimerized insulator whose gap is controlled by the amplitude of the dimerization order parameter: $\langle d_{i\alpha\sigma}^\dagger d_{i+1\alpha\sigma} - d_{i+1\alpha\sigma}^\dagger d_{i+2\alpha\sigma} \rangle + \text{H.c.}$ (the index i denotes the sites of a V chain oriented along the α direction). This exotic behavior of ZnV_2O_4 under pressure could be a more general characteristic of geometrically frustrated Mott insulators that approach the itinerant limit from the intermediate coupling regime. In general, highly frustrated Mott insulators tend to exhibit simultaneous *bond and magnetic* orderings in their strong coupling limit.^{19,20} The bond ordering emerges from the frustrated nature of the underlying lattice: there are different ways of choosing the frustrated bonds in the magnetically ordered ground state (a bond is "frustrated" if it connects two moments that are aligned in a single-bond high energy state). This freedom leads to a discrete broken symmetry in addition to the spontaneously broken symmetry of spin rotations that characterizes any magnetic ordering. Our study of ZnV_2O_4 suggests that these two orderings can become independent of each other away

from the strong-coupling regime. It is important to note that the coupling between the electronic and lattice degrees of freedom becomes stronger in the intermediate-coupling regime because the bond order parameter becomes of order one (it is of order t/U in the strong-coupling regime). This implies that a strong enough electron-phonon coupling can trigger the bond ordering in the absence of magnetic ordering. The stabilization mechanism is always the same: bonds that become inequivalent have different hopping amplitudes and this effect lowers the geometric frustration of the electronic kinetic energy terms.

The strengthening of the bond ordering away from the strong-coupling regime becomes particularly interesting when such ordering corresponds to a ferroelectric distortion, like in the case of CdV_2O_4 .¹³ Since the same structural distortion is observed in ZnV_2O_4 , our study suggests that the magnitude of the electric polarization and the ferroelectric Curie temperature can be increased significantly by decreasing the V-V distance. Moreover, the significant increase in the magnitude of the charge gap should also reduce the losses or leak currents that are the main limiting factor for measuring the spontaneous electric polarization of ZnV_2O_4 . Therefore, closing the Mott gap of geometrically frustrated Mott insulators is a potential route for enhancing electronically driven ferroelectricity. According to our results, this goal could be achieved in the spinel vanadates by reducing the V-V distance relative to the lattice parameter of ZnV_2O_4 . This should be done by a chemical substitution that does not introduce additional magnetic ions in order to preserve the

magnetic ordering of the AV_2O_4 family (with $A = \text{Cd, Mg, and Zn}$).

We acknowledge financial support from the DFG (SFB 484 and SFB 608) and the Bayerische Forschungsstiftung.

F.R. acknowledges support from Ministerio de Economía y Competitividad, Spain, through the project MAT2010-16157. Work at LANL was performed under the auspices of the US DOE Contract No. DE-AC52-06NA25396 through the LDRD program.

-
- ¹S. Blanco-Canosa, F. Rivadulla, V. Pardo, D. Baldomir, J. S. Zhou, M. Garcia-Hernandez, M. A. Lopez-Quintela, J. Rivas, and J. B. Goodenough, *Phys. Rev. Lett.* **99**, 187201 (2007).
- ²V. Pardo, S. Blanco-Canosa, F. Rivadulla, D. I. Khomskii, D. Baldomir, H. Wu, and J. Rivas, *Phys. Rev. Lett.* **101**, 256403 (2008).
- ³D. Baldomir *et al.*, *Physica B* **403**, 1639 (2008).
- ⁴H. Tsunetsugu and Y. Motome, *Phys. Rev. B* **68**, 060405(R) (2003).
- ⁵Y. Kato, G.-W. Chern, K. A. Al-Hassanieh, N. B. Perkins, and C. D. Batista, *Phys. Rev. Lett.* **108**, 247215 (2012).
- ⁶S. Niziol, *Phys. Status Solidi A* **18**, K11 (1973).
- ⁷H. K. Mao, J. Xu, and P. M. Bell, *J. Geophys. Res. Atmos.* **91**, 4673 (1986).
- ⁸D. L. Heinz and R. Jeanloz, *J. Appl. Phys.* **55**, 885 (1984).
- ⁹F. D. Murnaghan, *Am. J. Math.* **59**, 235 (1937).
- ¹⁰G. Huber, K. Syassen, and W. B. Holzapfel, *Phys. Rev. B* **15**, 5123 (1977).
- ¹¹See Supplemental Material at <http://link.aps.org/supplemental/10.1103/PhysRevB.86.020405> for detail of the phonon splitting and the pressure dependence across the structural transition. Resistivity vs temperature curves, at different pressures, and the corresponding fittings to extract the activation energy.
- ¹²M. Reehuis, A. Krimmel, N. Büttgen, A. Loidl, and A. Prokofiev, *Eur. Phys. J. B* **35**, 311 (2003).
- ¹³G. Giovannetti, A. Stroppa, S. Picozzi, D. Baldomir, V. Pardo, S. Blanco-Canosa, F. Rivadulla, S. Jodlauk, D. Niermann, J. Rohrkamp, T. Lorenz, S. Streltsov, D. I. Khomskii, and J. Hemberger, *Phys. Rev. B* **83**, 060402(R) (2011).
- ¹⁴Y. Kato and N. Kawashima, *Phys. Rev. E* **79**, 021104 (2009).
- ¹⁵Y. Kato, [arXiv:1202.5366](https://arxiv.org/abs/1202.5366) (to be published).
- ¹⁶Y. Kato, G.-W. Chern, N. B. Perkins, and C. D. Batista (in preparation).
- ¹⁷T. Maitra and R. Valenti, *Phys. Rev. Lett.* **99**, 126401 (2007).
- ¹⁸H. Tsunetsugu and Y. Motome, *Phys. Rev. B* **68**, 060405 (2003).
- ¹⁹S. E. Sebastian, N. Harrison, C. D. Batista, L. Balicas, M. Jaime, P. A. Sharma, N. Kawashima, and I. R. Fisher, *Nature (London)* **441**, 617 (2006); C. D. Batista, J. Schmalian, N. Kawashima, P. Sengupta, S. E. Sebastian, N. Harrison, M. Jaime, and I. R. Fisher, *Phys. Rev. Lett.* **98**, 257201 (2007); J. Schmalian and C. D. Batista, *Phys. Rev. B* **77**, 094406 (2008).
- ²⁰Y. Kamiya, N. Kawashima, and C. D. Batista, *Phys. Rev. B* **84**, 214429 (2011); R. M. Fernandes, A. V. Chubukov, J. Knolle, I. Eremin, and J. Schmalian, *ibid.* **85**, 024534 (2012).